This is a repository copy of *Controlled dual drug release from adhesive electrospun patches for prevention and treatment of alveolar osteitis*.

White Rose Research Online URL for this paper:
https://eprints.whiterose.ac.uk/218500/

Version: Published Version

Controlled dual drug release from adhesive electrospun patches for prevention and treatment of alveolar osteitis

Klaudia M. Slowik [a], Jake G. Edmans [a,b], Samuel Harrison [b], Sean M. Edwards [c], Robert Bolt [a], Sebastian G. Spain [b], Paul V. Hatton [a,d], Craig Murdoch [a,d,*], Helen E. Colley [a,d]

[a] School of Clinical Dentistry, 19 Claremont Crescent, University of Sheffield, Sheffield S10 2TA, UK
[b] Department of Chemistry, Brook Hill, University of Sheffield, Sheffield S3 7HF, UK
[c] Department of Mathematical Sciences, University of Liverpool, Liverpool L69 7ZL, UK
[d] Insigneo, University of Sheffield, Sheffield, UK

ARTICLE INFO

ABSTRACT

Approximately one in five individuals experience alveolar osteitis (AO) following wisdom tooth extraction. AO is characterised by loss of the blood clot from the tooth extraction socket leading to infection and pain, resulting in repeated hospital visits that impose a substantial burden on healthcare systems. Current treatments are sub-optimal; to address this we developed a novel drug-loaded mucoadhesive patch composed of dual electrospun polyvinyl pyrrolidone/Eudragit RS100 (PVP/RS100) and poly(*N*-isopropylacrylamide) (PNIPAM) fibres protected by a poly(ε-caprolactone) (PCL) backing layer. These patches demonstrated controlled release of the long-acting analgesic bupivacaine HCl and the anti-inflammatory drug prednisolone. Topical application of patches to tissue-engineered gingival mucosa showed that patch-released bupivacaine and prednisolone achieved sustained tissue permeation with 54.8 ± 3.3 % bupivacaine HCl and 65.8 ± 5.1 % prednisolone permeating the epithelium after 24 h. The drugs retained their functionality after release; bupivacaine HCl significantly ($p < 0.05$) inhibited veratridine-induced intracellular calcium flux in SH-SY5Y neuronal cells, while prednisolone significantly reduced gene expression of IL-6 (2-fold; $p < 0.001$), CXCL8 (5.1-fold; $p < 0.01$) and TNF-α (1.5-fold; $p < 0.001$) in stimulated THP-1 monocytes. Taken together, these data show that dual electrospun patches have the potential to provide a mucoadhesive covering to prevent blood clot loss while delivering pain relief and anti-inflammatory therapeutics at tooth extraction sites to prevent and treat AO. This study not only offers a future therapeutic pathway for AO but also contributes valuable insights into future advancements in drug delivery devices for periodontal or oral mucosal tissue.

1. Introduction

Alveolar osteitis (AO), commonly referred to as 'dry socket' poses a significant challenge in dental practice, often complicating tooth extraction procedures. The condition arises when the blood clot that forms in the tooth socket post-extraction becomes dislodged or disintegrates prematurely, exposing the underlying alveolar bone [1]. This exposure leads to acute and persistent pain and inflammation that prolongs the healing process, causing distress to patients [2]. Tooth extractions are the among the most common surgeries. For example, over 3.3 million of these procedures were performed in England in 2022–23 [3], while in the US around 10 million third molar (wisdom) tooth extractions are performed annually [4]. The reported incidence of

AO is up to 5 % of all routine extractions but this increases to 30 % for wisdom tooth extractions [5]. Therefore, AO is a considerable clinical problem.

Although the precise aetiology remains elusive, several risk factors such as smoking [6], age, gender [7], oestrogen levels [8] and oral health [9] are all known to have an impact. The incidence of AO is most common in the lower third molar teeth due to denser alveolar bone, which is associated with reduced vascularisation [1]. Current clinical guidelines for the management of AO recommend irrigation of the post-extraction tooth socket to remove debris and necrotic tissue without blood clot dislodgement, followed by the application of an intra-socket dressing such as Alveogyl or zinc oxide eugenol (ZOE) for temporary pain relief, with longer term pain management typically involving a

combination of analgesics, such as paracetamol and non-steroidal anti-inflammatory drugs (NSAIDs) [10]. SaliCept, a freeze-dried pledget containing an acemannan hydrogel derived from *aloe vera* that is applied intra-socket, has also been found to reduce incidence of AO [11]. However, the efficacy of these interventions is limited, and patients may require multiple visits for irrigation and dressing changes as the socket heals. Moreover, Alvogyl and ZOE contain eugenol that has been reported to cause hypersensitivity reactions as well as bone necrosis that may delay healing of the extraction socket [2,12]. Treatment with platelet-rich fibrin or low-level laser therapy offer promising alternatives in reducing AO and improving healing outcomes [13,14]. However, conflicting evidence and variability in study findings underscore the need for further research to establish their efficacy [15,16].

Antibiotics were previously advocated for AO prevention but there is a lack of robust evidence to support their routine use, especially given the increasing risk of antimicrobial resistance [17,18]. Chlorhexidine mouthwash, a commonly used antiseptic, has shown some efficacy in reducing AO incidence [19]. Prevention strategies aimed at mitigating the risk of clot dislodgement to promote optimal healing would be highly beneficial. To this end, the utilisation of a protective membrane to cover the post-extraction socket has shown promising outcomes.

Oxidised cellulose membranes have proved effective by stabilising the blood clot within the socket [20]. While, collagen membranes have shown to support wound healing by stabilising clots and possessing haemostatic properties [21]. A disadvantage of these systems is that they require suturing which is technically demanding and extends clinical time making it more expensive.

Recently, we have developed an electrospun mucoadhesive patch for targeted delivery of the anti-inflammatory corticosteroid, clobetasol-17-propionate, for the treatment of inflammatory oral mucosal diseases [22,23] and lidocaine for pain management [24]. The patch formulation utilises polyvinyl pyrrolidone (PVP)/Eudragit RS100 (RS100) as drug-loaded, fibre-forming polymers that demonstrate rapid drug release profiles [25]. The patch also comprises a hydrophobic backing layer of poly(ε-caprolactone) (PCL) to protect the mucoadhesive layer against mechanical forces, saliva and to ensure unidirectional delivery of drugs into the mucosa [23]. These microfibre patches are fabricated using electrospinning technology, where monoaxial electrospinning, the production of a homogeneous fibre patch from a single polymer mixture, is most common. However, incorporation of heterogeneous polymers fibres into a patch can be achieved using coaxial, triaxial, side-by-side/Janus or multi-jet techniques [26,27,28].

Inclusion of additional polymers in the fabrication process offers tailorability for longer-term adhesion with sustained release properties. Poly(*N*-isopropylacrylamide) (PNIPAM) is a thermoresponsive polymer with excellent electrospinning qualities [29,30] that has gained attention for controlled drug release [31]. PNIPAM is water soluble below its lower critical solution temperature of approximately 32 °C [32]. However, at physiological temperatures close to 37 °C electrospun PNIPAM forms a relatively hydrophobic hydrogel that is suitable for efficient and sustained drug release over several hours [33,34]. Electrospun technologies clearly have wider potential applications in oral medicine and dentistry, including in the development of new sustained drug delivery devices for treatment of AO as predicted by Edmans et al [35].

Herein, we successfully incorporated bupivacaine HCl, tramadol HCl (analgesics), celecoxib, naproxen (COX-2 inhibitor; NSAID) or prednisolone (corticosteroid) into PVP/RS100 electrospun mucoadhesive patches. These patches demonstrated rapid release of prednisolone and bupivacaine HCl. To control drug release, prednisolone-loaded PVP/RS100 fibres were electrospun in conjunction with bupivacaine HCl-loaded PNIPAM polymer fibres. In the dual electrospun patch, PNIPAM fibres produced sustained release of bupivacaine while simultaneously inducing controlled release of prednisolone from the PVP/RS100 fibres, without affecting patch adhesion. The drugs released from the dual electrospun patch permeated human tissue engineered gingival mucosal equivalents and retained their anaesthetic activity while suppressing a leukocyte-mediated inflammatory response. These patches will deliver both anti-inflammatory and anaesthetic therapeutics directly to the post-extraction site in a controlled manner whilst simultaneously retaining the blood clot in place, signifying a potential step-change in the prevention and treatment of AO.

2. Material and methods

2.1. Materials

All reagents were purchased from Merck (Gillingham, UK) unless otherwise stated. PVP (MW 2000 kDa) and RS100 (MW 38 kDa) were kindly donated by BASF (Cheadle Hulme, UK) and Evonik Industries AG (Essen, Germany), respectively.

2.2. Poly(N-isopropylacrylamide) synthesis

PNIPAM was synthesised by free radical precipitation polymerisation. *N*-isopropylacrylamide (NIPAM) (37 g, 0.33 mol) was dissolved in water (335 mL) and degassed with N_2 for 30 min. Ammonium persulfate (0.37 g, 1.6 mmol) dissolved in water was degassed with N_2 for 30 min then introduced to the NIPAM solution resulting in a 10 % *w*/w solid solution that was retained in an oil bath at 70 °C for 16 h. NIPAM conversion to PNIPAM was approximated at 100 % using ^{1}H NMR spectroscopy. The impure PNIPAM solid was freeze-dried and dissolved in tetrahydrofuran (THF), followed by precipitation into a ten-fold excess of petroleum ether at 40–60 °C and the resultant white PNIPAM powder (35 g) subjected to drying under reduced pressure. Gel permeation chromatography (GPC) of synthesised PNIPAM was performed in HPLC-grade DMF (0.1 mg/mL LiBr) using an Agilent 1260 Infinity Series degasser and pump, an Agilent PL-gel guard column, two Agilent Mixed-C columns, a refractive index detector and a UV detector set at a wavelength of 305 nm. The equipment was calibrated using eleven near-monodisperse poly(methyl methacrylate) standards (2.38×10^2–2.20×10^6 g/mol). Molar mass and dispersity were calculated with Agilent GPC software as $M_n = 915$ kg/mol and $M_w/M_n = 2.40$ (Supplementary Fig. 1).

2.3. Electrospinning system and fabrication of mucoadhesive dual and layer-by-layer electrospun patches

Electrospun patches were fabricated using a system comprising a PHD2000 syringe pump (Harvard Apparatus, Cambridge, UK) and an Alpha IV Brandenburg power source (Brandenburg UK Ltd., Worthing, UK) as previously described [23]. Plastic syringes (1 mL volume; Henke Sass Wolf, Tuttlingen, Germany) were used to drive the solutions into a 15-gauge blunt metallic needle (Fisnar Europe, Glasgow, UK). Mucoadhesive membranes were electrospun as previously described from solutions containing PVP (10 % *w*/w) and Eudragit RS100 (12 % *w*/w) in 97 % *v*/v ethanol and 3 % water [23]. PVP and RS100 were added to ethanol and mixed at room temperature using a magnetic stirrer until dissolved. The drugs: bupivacaine HCl, celecoxib, naproxen, prednisolone or tramadol HCl were added to the polymeric solution, contributing to 3 % w/w of the final dry patch composition, mixed until homogenous and incubated for 18 h to allow dissolution of the polymers and drugs. Placebo patches were prepared without the addition of the drugs. Electrospinning was performed at 18 °C, 45 % humidity at 19 kV, a flow rate of 2 mL and a flight path of 14 cm, utilising a flat collector.

PNIPAM (5 % *w*/v) was dissolved in a blend of chloroform and methanol (9:1 *v*/v) and stirred using a magnetic bar for 12 h at room temperature. Bupivacaine HCl was added to the polymeric solution, contributing to 3 % w/w of the final dry patch composition and mixed briefly until homogenous. Following optimisation (Supplementary Table 1), electrospinning was performed at 18 °C at 17 kV, a flow rate of 1 mL/h and a flight path of 14 cm, utilising a flat collector.

The dual electrospun patch consisted of two types of fibres: PVP (10

% *w/v*) combined with RS100 (12 % w/v) in 97 % v/v ethanol loaded with prednisolone (3 % *w/w*) and PNIPAM (5 % w/v) in chloroform and methanol (9:1 *v/v*) loaded with bupivacaine HCl (3 % w/w). Electrospinning was performed at 18 °C at 17 kV, a flow rate of 1 mL and a flight path of 14 cm, this time utilising a mandrel (rotating drum) collector rotating at 100 rpm. If a semi-solid substance formed around the nozzle of the spinneret, electrospinning was halted, the nozzle cleaned and then the process was restarted.

The final mucoadhesive electrospun patch consisted of three layers. The first layer being a dual electrospun layer consisting of PVP/RS100/prednisolone and PNIPAM/bupivacaine. With a lower polymer concentration (5 % PNIPAM compared to 10 % PVP/12 % RS100), electrospinning both blends under identical conditions generated less PNIPAM deposition compared to PVP/RS100. Therefore, to enhance bupivacaine content, the PNIPAM/bupivacaine layer required extended

electrospinning, forming a secondary layer. A final backing layer was made from electrospun PCL (10 % w/v) dissolved in a blend of dichloromethane (DCM) and dimethylformamide (DMF) (9:1 v/v). The resulting materials were placed in a dry oven at 70 °C for 20 min to melt the PCL layer into a continuous film [23]. A schematic representation of the electrospun patch fabrication process and how this was tested is provided in Fig. 1.

2.4. Scanning electron microscopy

Electrospun samples were mounted on 25 mm aluminium stubs and gold sputtered for 90 s with a 30 mA current. A Tescan Vega3 LMU scanning electron microscope (SEM) was used to image samples using an emission voltage of 10 kV. Fibre diameter was measured using ImageJ Software (National Institute of Health, US). Each fibre was randomly
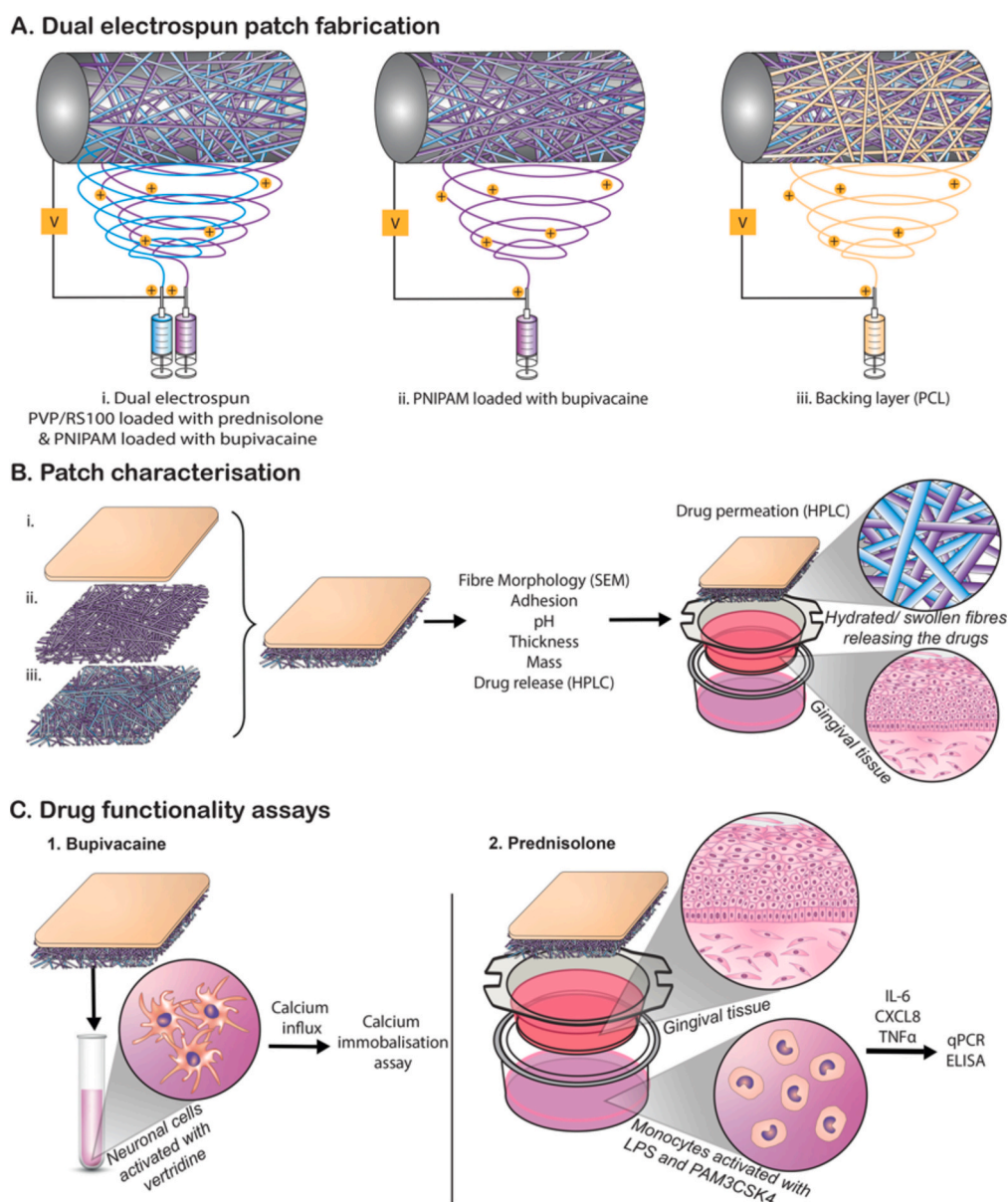
Fig. 1. Schematic illustration of patch fabrication and experimental design. The first layer was a blend of dual electrospun PVP/RS100 fibres loaded with prednisolone in conjunction with PNIPAM loaded with bupivacaine HCl. The middle layer consisted of PNIPAM loaded with bupivacaine HCl alone, required to increase the bupivacaine content. The final layer consisted of heat-treated PCL to provide a hydrophobic backing (A). Patches were extensive characterised and drug release measured in PBS and through in vitro gingival epithelium (B). Drug functionality was assessed upon release from patch: inhibition of voltage-gated sodium channels by bupivacaine was assessed using an intracellular calcium mobilisation assay (C1) while the anti-inflammatory effects of prednisolone was examined in LPS/PAM3CSK4-stimulated THP-1 monocytes (C2).

selected through generation of coordinates on a superimposed grid on an image ($n = 3$ patches, n = 3 images per patch, 10 fibre measured per image).

2.5. Conductivity of polymer solution

Conductivity of pre-electrospun polymers was measured using a Mettler Toledo FG3 conductivity meter, calibrated with a conductivity standard 1413 μS/cm. Between each use the conductivity meter was washed with solvent and deionised water.

2.6. Determination of patch thickness, mass uniformity, pH and adhesion

An electronic digital balance was used to measure patch mass while thickness was measured at three randomly selected points using Vernier callipers. For determination of pH, 10 mg patches were immersed in 5 mL of distilled water for 24 h and the pH measured using an electronic pH meter. To measure adhesion, patches (Ø 15 mm) were applied to wells of a 12-well plate containing 20 μL of PBS with gentle pressure for 5 s and then the wells flooded with 1 mL of PBS and placed on a thermo-shaker at 250 rpm at 37 °C. The patches were monitored for up to 180 h and the detachment time recorded.

2.7. Fabrication and imaging of dual fibre electrospun patches

To assess the incorporation of both PVP/RS100 and PNIPAM into the same electrospun patch, a fluorescent dye was added to each of the polymeric solutions at the preparation stage. 7-hydroxy-4-(trifluoromethyl) coumarin (0.015 % *w/v*) was added to the PVP/RS100, while PNIPAM was doped with Rhodamine 110 chloride (0.015 % w/v). Polymer solutions were electrospun into dual fibre patches onto glass coverslips as previously described [36] and imaged using a Zeiss LSM880 AiryScan confocal microscope or a Thunder 3D assay imager with RFID. All images were processed using ImageJ software tools.

2.8. Release profile of bupivacaine hydrochloride and prednisolone from electrospun patches

Three independently prepared electrospun patches (Ø 15 mm) containing bupivacaine HCl and prednisolone without the backing layers were weighed and submerged in 2 mL PBS in a 12-well plate at either 15 °C or 37 °C with shaking and 200 μL samples collected over time. Each 200 μL sample taken was replaced with the equivalent volume of fresh PBS. The presence of bupivacaine HCl and prednisolone was detected by reverse-phase high-performance liquid chromatography (RP-HPLC) with UV detection using an AXBridge BEH-C18 column (4.6 mm × 250 mm; 130 Å pore size), with a mobile phase of acetonitrile: water (3:7 *v/v*) containing 0.1 % trifluoroacetic acid (*v/v*) and a flow rate of 1 mL/min and a 10 μL injection volume. The detection wavelength was 201 nm and 245 nm for bupivacaine HCl and prednisolone, respectively. The retention time was 9.1 min for bupivacaine HCl and 7.9 min for prednisolone. The method was validated in terms of linearity and precision using bupivacaine HCl and prednisolone standards ranging from 39 to 250 μM. Percentage release of bupivacaine HCl and prednisolone was calculated from measured sample concentrations using Eq. (1) below. At each timepoint (T) the percentage release is the mass (M) permeated (present in PBS and lost to previous sampling) divided by the applied dry mass fraction of drugs in the electrospinning solution. Mass is related to concentrations (C) and volumes (V) via standard molar relations.

$$\%_{Released} = \frac{M_{PBS} + M_1 + M_2 + \cdots + M_{T-1}}{M_{Applied}}$$
$$= \frac{V_{PBS}C_{T} + V_{Sample}(C_1 + C_2 + \cdots C_{T-1})}{V_{Applied}C_{Applied}} \quad (1)$$

2.9. Cell culture

Immortalised human gingival keratinocytes, OKG4/bmi1/TERT (herein referred to as OKG4), were a gift from Prof. James Rheinwald [37]. OKG4 were maintained in K-FSM medium supplemented with bovine pituitary extract (BPE) (25 μg/mL), epidermal growth factor (EGF) (0.2 ng/mL), CaCl₂ (0.4 mM), penicillin (100 IU/mL) and streptomycin (100 μg/mL). The medium was changed every 2–3 days. For greater cell yields, OKG4 cells were cultured in K-SFM and D-FK medium mixed at 1:1 v/v ratio. D-FK medium consisted of high glucose Dulbecco's modified Eagle's medium (DMEM) and Ham's F12 (1:1 *v/v*) supplemented with ʟ-glutamine (2 mM), BPE (25 μg/mL), EGF (0.2 ng/mL), CaCl₂ (0.3 mM), penicillin (100 IU/mL) and streptomycin (100 μg/mL). Immortalised human gingival fibroblasts (HGF; Applied Biological Materials Inc., Richmond, BC, Canada) (da Cruz et al., 2020) were cultured in DMEM supplemented with foetal calf serum (FCS) (10 % v/v), ʟ-glutamine (2 mM), penicillin (100 IU/mL), and streptomycin (100 μg/mL). THP-1, a monocyte cell line isolated from the peripheral blood from an acute monocytic leukaemia patient [38], were cultured as a suspension in RPMI-1640 medium supplemented with FCS (10 % v/v), ʟ-glutamine (2 mM), penicillin (100 IU/mL), and streptomycin (100 μg/mL). The human neuroblastoma cell line SH-SY5Y (LGC Standards, UK) [39] were cultured in DMEM and Ham's F12 medium (1:1 v/v) supplemented with FCS (10 %, v/v), nonessential amino acids (1 %, v/v), ʟ-glutamine (2 mM), penicillin (100 IU/mL), and streptomycin (100 μg/mL).

2.10. Generation of oral epithelial equivalents

To generate reconstituted human gingival epithelial equivalents (RHGE), OKG4 were seeded onto the apical surface of Geltrex™-coated (10 μg/mL) 12-well, transwell inserts at 5×10^5 cells in 500 μL of K-SFM medium. After 2 days culture, RHGE were raised to an air-to-liquid interface (ALI) and the growth medium changed to differentiation medium consisting of DMEM and Ham's F12 medium (3:1 *v/v*) supplemented with FCS (10 % v/v), EGF (2 ng/mL), hydrocortisone (2 mM), insulin (0.1 mM), isoproterenol (1 mM), carnitine (10 mM), ʟ-ascorbic acid (0.4 mM), ʟ-serine (10 mM), penicillin (100 IU/mL), streptomycin (100 μg/mL) and amphotericin B (0.625 μg/mL) as previously described [40]. RHGE were cultured at ALI for 7 days, with medium changes every 2–3 days.

Full thickness tissue engineered human gingival mucosal equivalents (GME) were constructed as previously described [40]. In brief, HGF were mixed with rat tail type I collagen (2.5×10^5 HGF/mL collagen), and 1 mL added to 12-well, 0.4 μm pore transwell ThinCerts™ (Greiner Bio One Ltd., Stonehouse, UK) and left to set at 37 °C in a humidified atmosphere for 30 min. Once set, OKG4 were seeded topically at a density of 5×10^5 cells in 500 μL of K-SFM. After 2 days, GME were raised to an ALI, the medium changed to differentiation medium and cultured for 7 days, with the medium changed every 2–3 days.

2.11. Lactate dehydrogenase release assay

Cell damage was assessed by quantifying the release of lactate dehydrogenase (LDH) into the culture medium, employing the CytoTox96 enzyme assay kit according to the manufacturer's instructions (Promega, Madison, WI). SDS (5 % v/v) was used as a positive control.

2.12. Transepithelial electrical resistance

To assess RHGE and GME integrity, transepithelial electrical resistance (TEER) was measured using an EVOM2 voltmeter at three distinct locations within each model. The epithelial resistance was determined by subtracting the resistance value derived from an empty cell culture insert and TEER value calculated using Eq. (2) below:

$$\text{TEER}\left(\Omega \cdot cm^2\right) = \text{Resistance}\left(\Omega\right) \times \text{Membrane area}\left(cm^2\right) \tag{2}$$

2.13. Drug permeation through reconstituted human gingival epithelial equivalents

Prednisolone or bupivacaine HCl-loaded patches were cut into 12 mm diameter disks and weighed. To facilitate patch adhesion, the surface of RHGE within transwells were moistened with 20 μL PBS, and the patch applied with forceps. Control RHGE received prednisolone or bupivacaine HCl in a PBS solution equivalent to the patch content (120 μg in 500 μL) or PBS alone. RHGE was placed in 12-well plates containing 1 mL of PBS as a receptive medium and incubated in a humidified atmosphere (95 % air, 5 % CO2) at 37 °C with agitation at 100 rpm. Samples (200 μL) were removed from the receptive medium and replaced with an equivalent volume of PBS for up to 24 h. The samples were stored at −80 °C before analysis by RP-HPLC and the accumulative drug permeation calculated using Eq. (1).

2.14. Bupivacaine hydrochloride functional assay

SH-SY5Y cells were loaded with the fluorescent calcium indicator Fluo-4 Direct following the manufacturer's instructions. Briefly, cells were removed from tissue culture flasks using ethylenediaminetetraacetic acid, centrifuged at 220 g for 5 min and resuspended at 10^6 cells/mL in a Fluo-4 Direct calcium buffer for 1 h at 37 °C. To test bupivacaine bioactivity, bupivacaine HCl-loaded or placebo electrospun patches were cut and for each 10 mg of patch, 1 mL of SH-SY5Y medium added and incubated for 24 h at 37 °C until fully dissolved, filter sterilised, then the solution added to Fluo-4-loaded cells to give a final concentration of 100 μg/mL (345 μM) bupivacaine for a further 1 h at room temperature. Eluate from the placebo patch or bupivacaine HCl solution (100 μg/mL) were used as controls. To determine intracellular calcium responses, fluorescence was measured at 488 nm excitation and 530/30 nm emission using a LSR II Flow Cytometer (BD Biosciences). For each sample, baseline fluorescence was measured for 10 s, then cells stimulated with veratridine or DMSO (vehicle control) and the fluorescence response measured for a further 120 s. Relative fluorescence units (RFU) were calculated by subtracting the baseline median fluorescence intensity from the maximal median fluorescence intensity following stimulation.

2.15. Prednisolone functional assay

Prednisolone and placebo patches (10 mg) were submerged in 1 mL of THP-1 culture medium (section 2.9) for 12 h at 37 °C and filter-sterilised before use. THP-1 cells were activated by incubating with 100 ng/mL utra-pure lipopolysaccharides (LPS) from *Escherichia coli* and 100 ng/mL Pam3CysSerLys4 (PAM3CSK4; Invivogen, Toulouse France), for 24 h at 37 °C. Following activation, THP-1 cells were centrifuged, and resuspended at a density of 1×10^6 cells/mL in either THP-1 growth medium alone (stimulated control), medium containing prednisolone eluted from the patch, medium containing eluate from the placebo patch or 100 μg/mL prednisolone dissolved in medium (positive control). THP-1 cells were harvested after 6 h for gene expression analysis and the condition medium collected after 24 h, stored at −80 °C then analysed by ELISA. To assess patch-delivered prednisolone permeation and activity in a 3D tissue, activated THP-1 cells were placed in the basolateral compartment of a well containing a GME within a transwell and a prednisolone-containing patch placed topically onto its surface. A placebo (non-medicated) patch, 100 μg/mL prednisolone solution (positive control) or growth medium alone (negative control) served as controls. GME were incubated for 24 h, after which THP-1 cells and the conditioned medium from the lower well was collected. RNA was extracted from THP-1 cells and analysed for gene expression by qPCR while ELISA was used to determine cytokine levels released into the conditioned medium (Fig. 1).

2.16. RNA isolation and reverse transcription-quantitative polymerase chain reaction (RT-qPCR) analysis

Total RNA from THP-1 cells was isolated using a Monarch® Total RNA Miniprep Kit (New England Biolabs, Frankfurt, Germany) according to the manufacturer's instructions. Total RNA (500 ng) was reverse transcribed using a high-capacity cDNA reverse transcription kit (Thermo Fisher Scientific), according to the manufacturer's instructions. qPCR analysis was conducted employing TaqMan gene expression assays. 0.5 μL of cDNA was amplified with 5 μL of master mixture, 3.5 μL of nuclease-free H_2O and 0.5 μL of TaqMan gene probe (FAM): IL-6 (Hs00174131), CXCL8 (Hs00174103), TNF-α (Hs01113624) and β2-microglobulin (VIC) as a reference control (Thermo Fisher Scientific). Thermal cycling included an initial step of 95 °C for 10 min, followed by 40 cycles of 10 s at 95 °C and 45 s at 60 °C. The threshold cycle was normalised against the β2-microglobulin reference gene and subsequent fold-changes in expression relative to the medium alone control group were determined using the formula $2^{-\Delta\Delta Ct}$.

2.17. Enzyme-linked immunosorbent assay

The concentration of IL-6, CXCL8, and TNF-α in conditioned media was evaluated by ELISA (R&D Systems, UK) following the manufacturer's instructions. Spectrophotometric readings were taken at 450 nm with a 570 nm correction filter using a Tecan Infinite M200 plate reader coupled with Magellan software.

2.18. Histological analysis

RHGE and GME were fixed in neutral-buffered formalin (10 % v/v) for 24 h and paraffin-wax embedded using standard histology procedures. Sections (5 μm) were cut using a Leica RM2235 microtome (Leica Microsystems, Wetzlar, Germany) and mounted on Superfrost Plus slides (Thermo Fisher Scientific, Loughborough, UK). Sections stained with haematoxylin and eosin were mounted in distyrene-polystyrene xylene and imaged by Olympus BX51 microscope with cellSens Imaging Software (Olympus GmbH, Hamburg, Germany).

2.19. Statistical analysis

All data and statistical analyses were performed using GraphPad Prism 10 software (GraphPad Software, La Jolla, USA). Unless otherwise indicated, all data are expressed as the mean ± standard deviation (SD). Statistically significant differences between two data sets were determined using unpaired Student's *t*-test or Mann Whitney *U* test. To determine statistical significance between multiple data sets, ordinary one-way ANOVA was employed followed by a Dunnett's or Tukey's post-hoc test for multiple comparisons to control for each other, respectively. Data were considered significant when $p < 0.05$.

3. Results

3.1. Incorporation of drugs into a mucoadhesive electrospun patch

Mucoadhesive electrospun patches containing bupivacaine HCl, celecoxib, naproxen, prednisolone and tramadol HCl (all at 3 % w/w) were produced by modification of our published protocol [23]. Before electrospinning, conductivity of the polymeric solutions was measured and compared to placebo (non-medicated) patches. The conductivity of the placebo polymeric solution (127.4 ± 2.17 μS/cm) were similar to when celecoxib (126.6 ± 0.78 μS/cm), naproxen (125.9 ± 1.66 μS/cm) and prednisolone (126.3 ± 1.76 μS/cm) were added (Fig. 2A). However, a significant increase in conductivity was observed for bupivacaine HCl (235 ± 1.53 μS/cm; $p < 0.001$) and tramadol HCl (273 ± 1.01 μS/cm; p < 0.001).

SEM images of the electrospun layer with and without drug
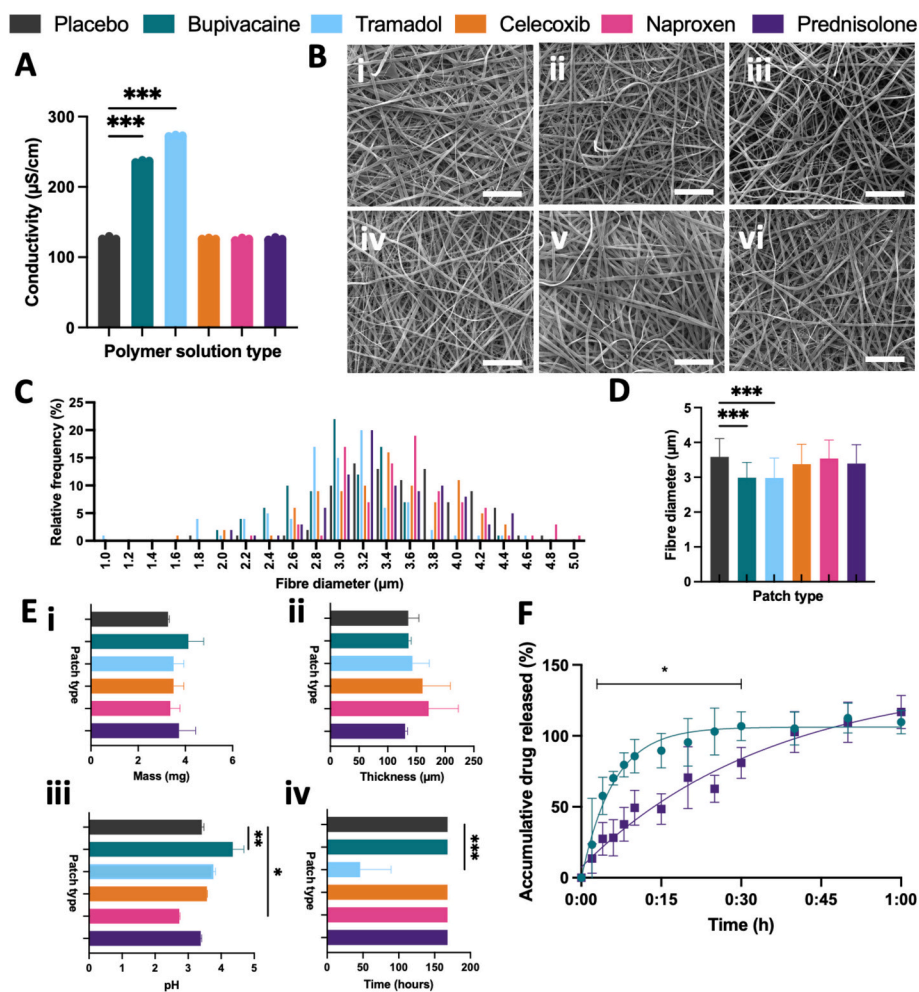
Fig. 2. Incorporation of analgesics and anti-inflammatory drugs into the mucoadhesive patch. Placebo (dark grey), bupivacaine HCl (teal), tramadol (blue), celecoxib (orange), naproxen (pink), or prednisolone (violet) were all incorporated at 3 % *w*/w. Conductivity measurements of the drug-doped polymeric solutions **(A)**. SEM images of the mucoadhesive fibres for placebo patch **(Bi)** and after incorporation of bupivacaine HCl **(Bii)**, tramadol HCl **(Biii)**, celecoxib **(Biv)**, naproxen **(Bv)** and prednisolone **(Bvi)**, scale bar = 50 μm. Relative fibre frequency diameter measurements, $n = 90$ **(C)** and average fibre diameters presented as mean ± SD, n = 90 **(D)**. Electrospun mucoadhesive patches were characterised for mass **(Ei)**, thickness **(Eii)**, pH **(E iii)** and adhesion to tissue culture plastic **(Eiv)**. Electrospun patches (10 mg) were submerged in PBS for 1 h and the accumulated drug release measured by RP-HPLC at increasing time intervals **(F)**. Data are shown as mean ± SD, $n = 3$, from three independent experiments. Statistical significance was determined using an ordinary one-way ANOVA followed by Dunnett's post-hoc test **(A, D and E)** and student *t*-test **(F)** with a significance difference indicated by *$p < 0.05$, **$p < 0.01$, ***$p < 0.001$. (For interpretation of the references to colour in this figure legend, the reader is referred to the web version of this article.)

incorporation revealed uniformly dispersed, randomly oriented fibres (Fig. 2B-D). The mean fibre diameter of the placebo patch was 3.58 ± 0.52 μm with no difference observed when loaded with celecoxib (3.37 ± 0.57 μm), naproxen (4.54 ± 0.53 μm) or prednisolone (3.39 ± 0.54 μm). In contrast, bupivacaine HCl (2.99 ± 0.44 μm; p < 0.001) and tramadol HCl (2.98 ± 0.57 μm; p < 0.001) demonstrated significantly narrower fibres when compared to the placebo (Fig. 2C-D).

Material characterisation revealed uniformity in mass and thickness across all drug-loaded patches (Fig. 2 Ei and ii). The pH of the placebo patch was 3.42 ± 0.07. In comparison, the pH for bupivacaine HCl (4.36 ± 0.33) doped patch was significantly increased while that of naproxen (2.74 ± 0.03) was significantly decreased (Fig. 2 Eiii). All patches were shown to adhere to tissue culture plastic for >168 h, except for tramadol HCl where adhesion was significantly reduced to 46 ± 43 h (p < 0.001) (Fig. 2 Eiv).

Following material characterisation and to match clinical practice, prednisolone and bupivacaine were taken forward for future experiments. Accumulative drug release from patches over 1 h revealed a rapid release of bupivacaine HCl, with approximately 85 % of the total drug being released within 10 min and 100 % by 25 min. Conversely,

prednisolone was more gradually released, with 49 % released by 10 min and 100 % after 40 min (Fig. 2F).

3.2. Use of poly(N-isopropylacrylamide) for the controlled release of bupivacaine hydrochloride

To meet clinical need, bupivacaine HCl should be released from the patch in a sustained manner, so that pain control is effective over a prolonged period. Therefore, we aimed to develop a PNIPAM formulation that could achieve a more sustained release of bupivacaine HCl. This formulation could then be employed in a dual electrospun patch. Pre-electrospun PNIPAM solution conductivity was 4.33 ± 0.005 μS/cm but once doped with bupivacaine HCl this significantly increased to 10.64 ± 0.19 μS/cm ($p = 0.002$) (Fig. 3A). SEM images of electrospun PNIPAM (5 % *w*/v) loaded with bupivacaine HCl (3 % *w*/w) revealed that the PNIPAM patches had uniformly dispersed, randomly oriented fibres with an average fibre diameter of 2.07 ± 0.38 μm. The addition of bupivacaine HCl (3 % w/w) to the PNIPAM fibres resulted in significantly narrower fibres (1.84 ± 0.37 μm; $p = 0.003$) (Fig. 3B-D).

Physicochemical testing revealed uniformity in mass and thickness
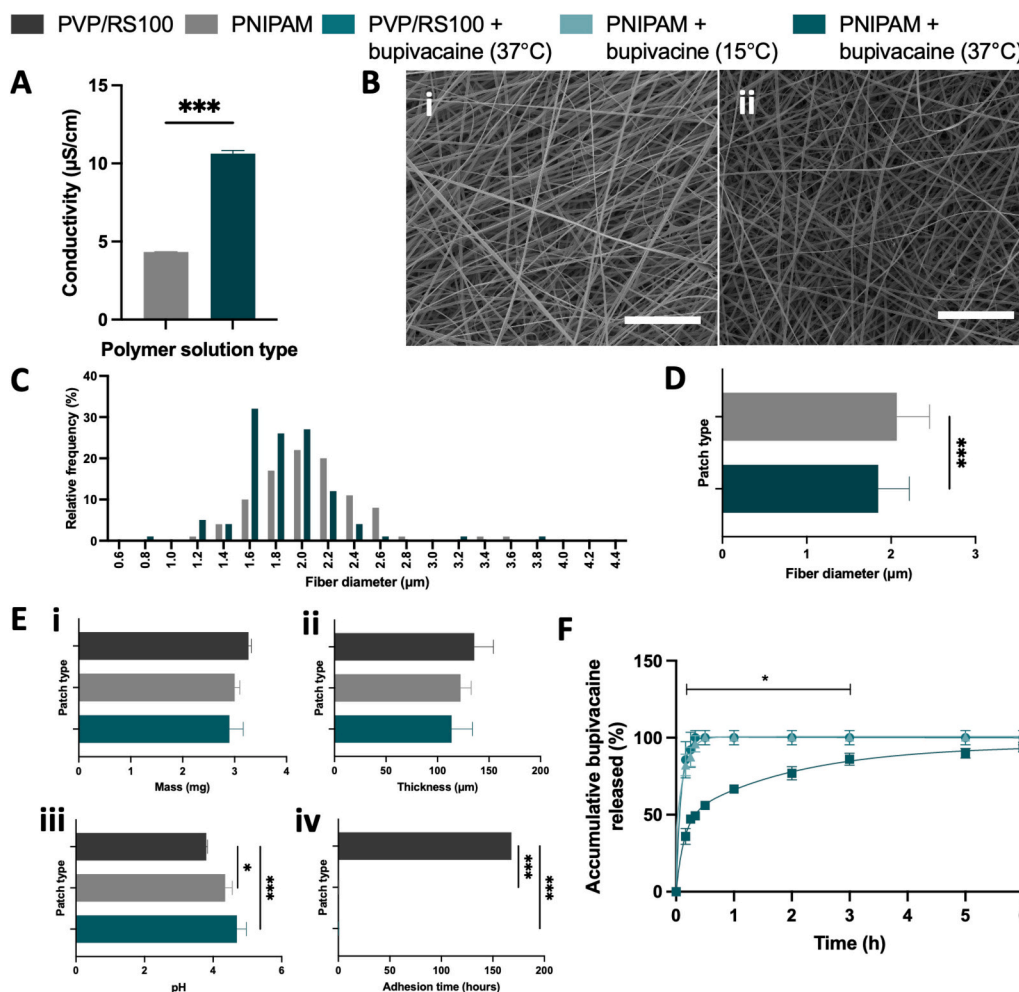
Fig. 3. Investigation of PNIPAM fibres, incorporation of bupivacaine HCl and release rates. PVP/RS100 + bupivacaine HCl (37 °C) (teal), PNIPAM (grey), PNIPAM + bupivacaine HCl (15 °C) (light teal) and PNIPAM + bupivacaine HCl (37 °C) (dark teal). Polymer solution measurements were taken using a conductivity meter **(A)**. SEM images of the fibres composed of PNIPAM **(Bi)** and PNIPAM with bupivacaine HCl **(Bii)**, scale bar = 50 μm. Relative fibre frequency diameter measurements, $n = 90$ **(C)** and average fibre diameters presented as mean ± SD, n = 90 **(D)**. Electrospun mucoadhesive patches were characterised for mass **(Ei)**, thickness **(Eii)**, pH **(Eiii)** and adhesion to tissue culture plastic, with no adhesion observed for PNIPAM and PNIPAM + bupivacaine HCl **(Eiv)**. Electrospun patches (10 mg) were submerged in phosphate-buffered saline (PBS) for 6 h and the accumulated drug release measured by RP-HPLC at increasing time intervals **(F)**. Data are shown as mean ± SD for $n = 3$, for three independent experiments. Statistical significance was determined using a student *t*-test **(A, D, F)** or an ordinary one-way ANOVA **(E)** followed by Dunnett's post hoc test with a significance difference indicated by * $p < 0.05$, *** $p < 0.001$. (For interpretation of the references to colour in this figure legend, the reader is referred to the web version of this article.)

across all patches (Fig. 3 Ei and ii). The pH of both the PNIPAM placebo and bupivacaine HCl-loaded patches were similar to each other but pH was significantly increased compared to PVP/RS100 patches (Fig. 3 Eiii, $P < 0.05$). In contrast to PVP/RS100 patches, PNIPAM patches were non-adhesive (Fig. 3 Eiv).

Bupivacaine HCl release profile from the PNIPAM fibres was determined at 15 °C and 37 °C. At 15 °C, the patch exhibited a similar rapid release profile to that of PVP/RS100 bupivacaine HCl-loaded patch at 37 °C, with 79 % of the drug released within 10 min and full release by 35 min. In contrast, when the PNIPAM patch was incubated at 37 °C, the fibres displayed slower release kinetics of bupivacaine HCl with 30 % of the drug content released in 10 min, increasing to 94 % by 6 h (Fig. 3F).

3.3. Dual electrospinning of polyvinyl pyrrolidone/Eudragit RS100 and poly(N-isopropylacrylamide) fibres for drug release

To investigate the incorporation of PVP/RS100 and PNIPAM fibres via dual electrospinning, polymer solutions were labelled fluorescent red (PVP/RS100) or green (PNIPAM). When both of the polymers were electrospun onto a flat collecting plate the fibres repelled each other

producing separate mat (Supplementary Fig. 2). Therefore, a mandrel collector was employed to promote intertwining of fibres, producing a homogenous electrospun mat that was confirmed by confocal microscopic analysis (Fig. 4A). SEM analysis of the final patch composition showed a tri-layer structure consisting of: 1) a dual fibre electrospun mat comprised of prednisolone (3 % *w/w*)-loaded PVP/RS100 fibres and bupivacaine HCl (3 % w/w)-loaded PNIPAM; 2) a bupivacaine HCl (3 % w/w)-loaded PNIPAM mat (to increase the overall bupivacaine HCl content; and 3) a PCL backing layer (Fig. 4 Bi-ii), with the different layers consecutively spun on top of one another. Once constructed, the resultant patch was exposed to heat treatment (20 min at 70 °C) in order to melt the PCL to form a water-resistant backing layer (Fig. 4B).

SEM images of the individual fibres in each patch showed that drug-containing fibres were a similar diameter to each other and their non-drug-containing counterparts, except PNIPAM + bupivacaine HCl which were smaller than PNIPAM fibres alone (p < 0.001) (Fig. 4C-E). Similarly, the dual electrospun patches, with and without drugs, displayed similar characteristics in terms of mass, thickness and pH to each other and the PNIPAM alone patches but these were all significantly lighter, thinner and with higher pH than PVP/RS100 patches (Fig. 4 Fi-
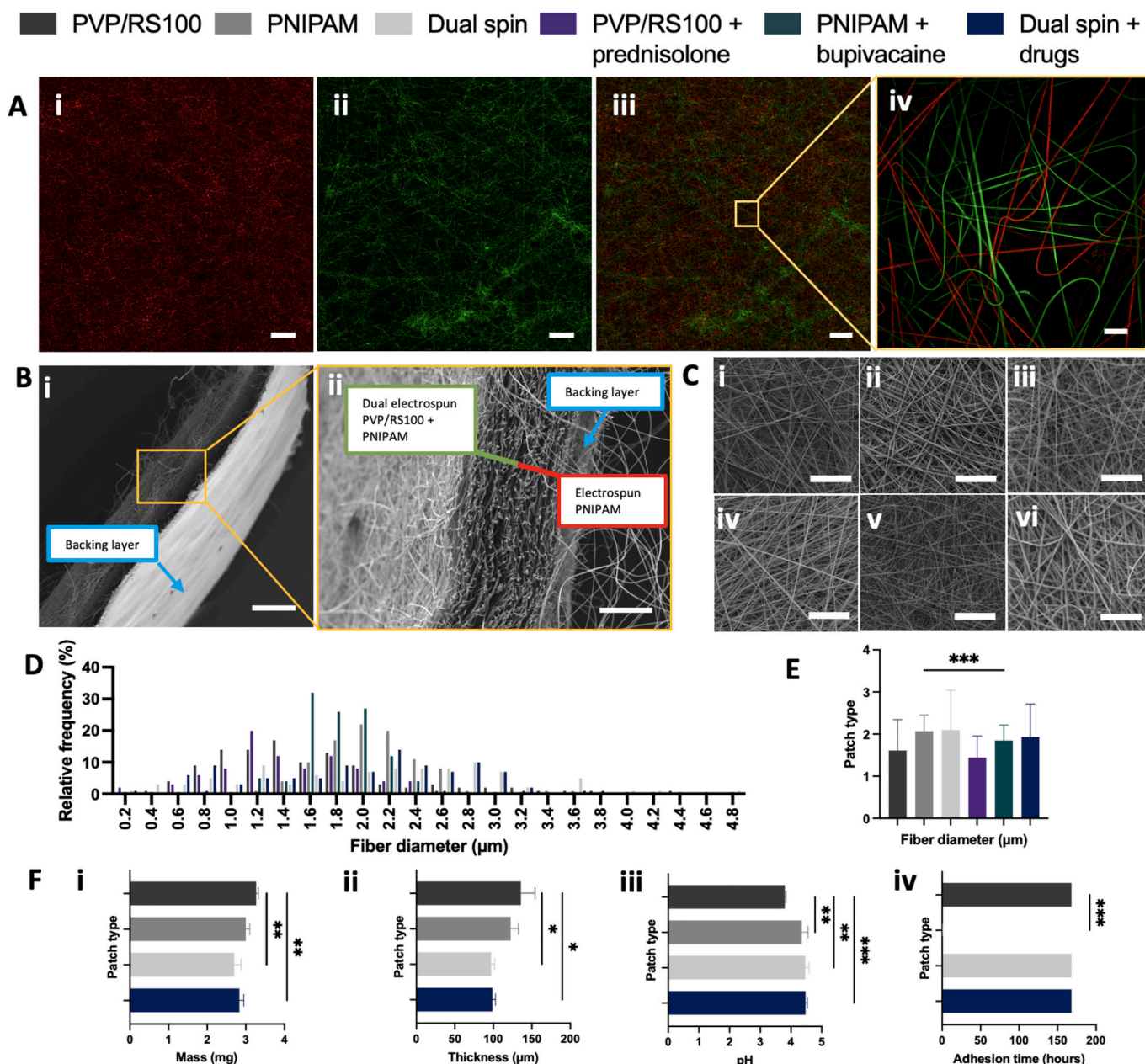
Fig. 4. Dual electrospun patch for controlled drug release. PVP/RS100 (dark grey), PNIPAM (grey), dual spin (light grey), PVP/RS100 + prednisolone (violet) PNIPAM + bupivacaine HCl (37 °C) (dark teal) and dual spin + drugs (navy). The dual spin consists of two different polymer blends: PVP/RS100 labelled with 7-hydroxy- 4(trifluoromethyl)coumarin (red), and PNIPAM labelled with rhodamine 110 chloride (green). Scale bar = 250 μm (Ai-iii) and 25 μm **(Aiv)**. SEM cross section images of the final patch formulation, revealing the tri-layer composition **(Bi-ii)**. The first layer consists of dual electrospun PVP/RS100 doped with prednisolone and PNIPAM loaded with bupivacaine HCl, the second layer is composed of PNIPAM doped with bupivacaine HCl, and the backing layer is composed of PCL. SEM images of the mucoadhesive fibres for PVP/RS100 **(Ci)**, PNIPAM **(Cii)**, dual spin **(Ciii)**, PVP/RS100 and prednisolone **(Civ)**, PNIPAM and bupivacaine HCl **(Cv)** and dual spin loaded with bupivacaine HCl and prednisolone **(Cvi)**. Relative fibre frequency diameters measurements, $n = 90$ **(D)** and fibre diameters are shown as mean ± SD, n = 90 **(E)**. Electrospun mucoadhesive patches were characterised for mass **(Fi)**, thickness **(Fii)**, pH **(Fiii)** and adhesion to tissue culture plastic **(Fiv)**. Data are shown as mean ± SD $n = 3$, for three independent experiments. Statistical significance was determined using an ordinary one-way ANOVA followed by Dunnett's post hoc test with a significance difference indicated by $*p < 0.05$, $**p < 0.01$, $***p < 0.001$. (For interpretation of the references to colour in this figure legend, the reader is referred to the web version of this article.)

iii). Interestingly, dual spun fibres with or without drug as well as PVP/RS100 patches alone were highly adherent whereas PNIPAM patches alone were non-adherent, suggesting that adhesion of dual patches is via PVP/RS100 alone (Fig. 4 Fiv).

3.4. Drug release from the dual electrospun patch

The release kinetics of bupivacaine HCl into PBS was similar from patches composed entirely of drug-loaded PNIPAM and from dual spun patches that also contained prednisolone-loaded PVP/RS100 (Fig. 5 Ai). In contrast, release of prednisolone into PBS from dual spun patches that also contained bupivacaine HCl-loaded PNIPAM was significantly slower ($p = 0.002$ over the first 2 h) than release from patches composed entirely of drug-loaded PVP/RS100 (Fig. 5 Aii), suggesting that PNIPAM fibres slow down the release of prednisolone from PVP/RS100 fibres when these fibres are combined into one patch.
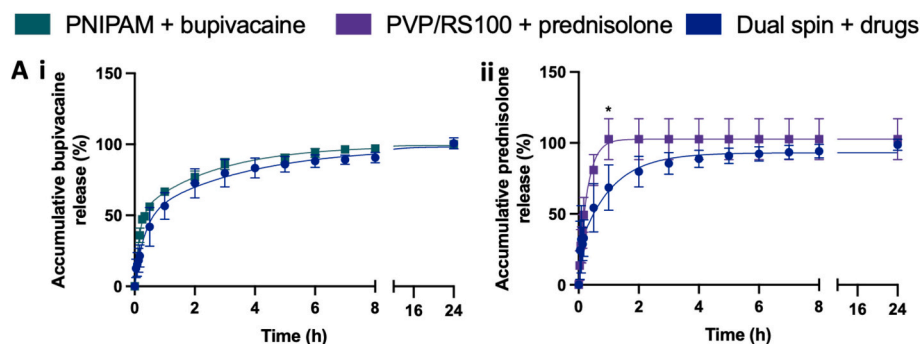
Fig. 5. Drug release from the dual electrospun patch. Dual spin + drugs (navy), PNIPAM + bupivacaine (dark teal), PVP/RS100 + prednisolone (violet). Electrospun patches (10 mg) were submerged in PBS and the accumulated drug release measured by RP-HPLC at increasing time intervals for bupivacaine HCl (Ai) and prednisolone (Aii). Data are shown as mean $\pm$ SD, n = 3, for three independent experiments. Statistical significance was determined using a student *t*-test with a significant difference indicated by *$p < 0.05$. (For interpretation of the references to colour in this figure legend, the reader is referred to the web version of this article.)

3.5. Topical application and permeation through reconstituted human gingival epithelial equivalents

We next examined permeation of drugs through RHGE when delivered topically via patch or in solution. The RHGE formed a multi-layered stratified squamous epithelium on polycarbonate membranes (Fig. 6 Ai) and displayed an excellent permeability barrier by day-7 culture as determined by TEER analysis (Fig. 6 Aii). A LDH assay was performed to confirm that the treatments were not cytotoxic. The placebo dual spin patch showed no difference in LDH release in comparison to the negative control, whereas the drug-loaded dual spin patch caused significantly lower LDH release ($p < 0.001$) compared to control (no patch) or dual patch alone controls, suggesting that inclusion of drugs into patches

resulted in less epithelial damage than controls (Fig. 6 Aiii).

The permeation of bupivacaine HCl and prednisolone released from a topically applied dual electrospun patch were compared to drugs in solution using RHGE (Fig. 6B). Drug permeation into and across RHGE was much slower than release directly into PBS. In the first 3 h no significant difference was observed in epithelial permeation between bupivacaine HCl in solution compared to that released from the dual patch. After 4 h, significantly more dual patch-released bupivacaine HCl permeated the epithelium (38.5 ± 4.3 %) than from solution (27.6 ± 1.7 %, $p < 0.05$) and this trend continued up to 24 h (54.8 ± 3.3 % patch compared to 35.8 ± 8.3 % solution, $p < 0.001$, Fig. 6 Bi).

A similar profile was observed for prednisolone. Here, drug permeation was similar for patch-released drug and that in solution for up to 3
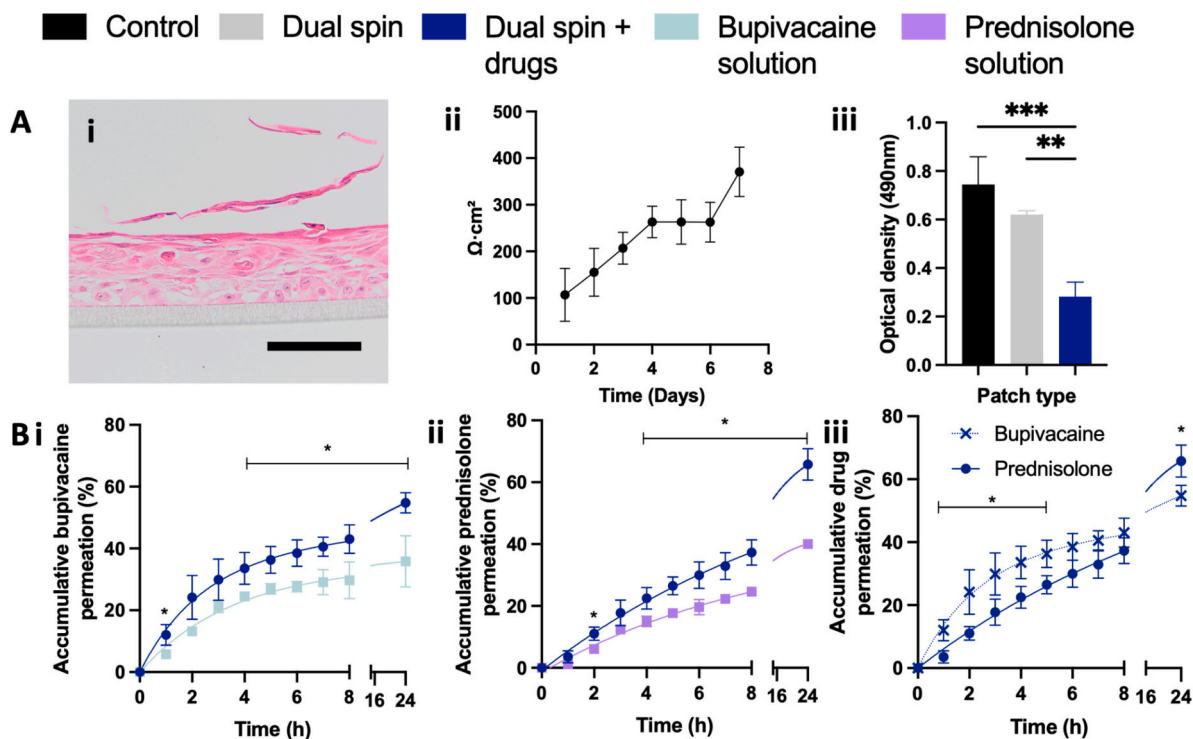
Fig. 6. Topical application and permeation through reconstituted human gingival epithelial equivalents. The permeation of drugs from the dual-spun path was assessed through RHGE; scale bar = 100 μm. **(Ai)**. TEER measurements were taken every day over a 7-day period to confirm permeability barrier **(Aii)**. LDH release indicating the cytotoxicity after 24 h treatment with dual spin drug-loaded patch with and without drug incorporation **(Aiii)**. RP-HPLC measured accumulative permeation of bupivacaine HCl **(Bi)** or prednisolone **(Bii)** from dual electrospun patch compared to drug in solution control, and accumulative permeation of bupivacaine HCl and prednisolone from dual electrospun patch **(Biii),** all after topical application for 24 h. Data are shown as mean $\pm$ SD, $n = 3$, for three independent experiments. Statistical significance was determined using an ordinary one-way ANOVA **(A)** followed by Tukey's post hoc or student *t*-test **(B)** test with a significant difference indicated by *$p < 0.05$, **$p < 0.01$, ***$p < 0.001$.

h. After 24 h 65.8 $\pm$ 5.1 % prednisolone had permeated the RHGE when released from the dual patch compared to only 40.0 $\pm$ 1.0 % permeation from the prednisolone applied in solution ($p < 0.001$) (Fig. 6 Bii). Permeation of bupivacaine HCl from PNIPAM fibres was significantly more rapid over the first 5 h compared to prednisolone from PVPS/RS100 fibres when applied as dual patches ($p < 0.01$, Fig. 6 Biii). Prednisolone ultimately achieved a higher epithelial permeation compared to the bupivacaine HCl at 24 h ($p < 0.05$, Fig. 6 Biii).

3.6. Bupivacaine hydrochloride released from electrospun patches blocks voltage-gated sodium channels and prevents veratridine- induced calcium responses in SH-SY5Y neuroblastoma cells

To confirm that bupivacaine HCl retained its analgesic activity once released from the dual patch, intracellular calcium flux measurements were used to establish functionality. Veratridine, causes persistent opening of voltage-gated sodium channels leading to cell depolarisation and downstream intracellular calcium flux [41]. Analgesics such as bupivacaine HCl have been shown to exert their biological action by blocking these voltage-gated sodium channels preventing veratridine-induced intracellular calcium flux [42]. The difference in the calcium flux in SH-SY5Y cells was measured post-veratridine treatment by incubation with elutes from patches or bupivacaine HCl in solution as control. Addition of veratridine caused a rapid intracellular calcium flux in untreated controls or cells preincubated with elute from placebo patches with relative fluorescence reaching 1624 $\pm$ 91 and 1009 $\pm$ 122, respectively. In contrast, SH-SY5Y cells pre-incubated with bupivacaine HCl in solution ($p < 0.01$) or as elute from a patch ($p < 0.05$) significantly reduced veratridine-induced intracellular calcium flux, showing that bupivacaine released from patches retained pharmacological activity by blocking voltage-gated sodium channels (Fig. 7A&B).

3.7. Anti-inflammatory effects of prednisolone following patch release

The biological action of prednisolone following elution from the drug-loaded dual electrospun patch was tested by its ability to suppress pro-inflammatory cytokine release in THP-1 monocytic cells following their stimulation with a combination of LPS (to mimic Gram-negative bacteria) and PAM3CSK4 (to mimic Gram-positive bacteria). Stimulated THP-1 cells were placed underneath a GME to represent patch-mediated prednisolone delivery more closely in inflamed post-

extraction tissue. Prednisolone was then applied to the top of the GME either as a drug-loaded patch or in solution for 24 h; a placebo non-medicated placebo patch was used as a negative control. Gene expression of the inflammatory cytokines IL-6, CXCL8 and TNF-α were measured in THP-1 cells and the levels of these cytokines secreted into the medium by both THP-1 and GME, measured by ELISA.

When stimulated by bacterial products (LPS & PAM3CSK) THP-1 increased IL-6 gene expression 2.6-fold compared to untreated controls ($p < 0.001$). Addition of eluate from the placebo patch increased expression further to 3.7-fold above baseline ($p < 0.001$). However, when treated with eluate from the prednisolone-loaded patch, IL-6 gene expression was significantly reduced to 2.0-fold ($p < 0.05$) which was consistent with the reduced IL-6 expression observed when treated with a solution of prednisolone (1.8-fold) (Fig. 8 Ai). The same trend was observed for the chemokine, CXCL8. Here, stimulated THP-1 cells displayed a 7.2-fold increase compared to untreated controls that was once again increased to 10.27-fold upon treatment with placebo elute. However, CXCL8 gene levels were significantly reduced following incubation with the elute from both the prednisolone patch (5.1-fold; $p < 0.01$) and prednisolone in solution (2.8-fold; $p < 0.001$) (Fig. 8 Aii). For TNF-α gene expression in THP-1 cells following stimulation significantly increased by 6.7-fold compared to unstimulated control. Interestingly, eluate from the placebo patch significantly reduced expression to 1.5-fold ($p < 0.001$). Gene expression levels were similarly decreased by treatment with elute from the prednisolone patch (0.75-fold; $p < 0.001$); and prednisolone in solution (1.4-fold; $p < 0.001$) (Fig. 8 iii).

Cytokine levels released into the medium mirrored those observed at the THP-1 gene expression level. For both IL-6, CXCL8 and TNF-α, secreted levels were significantly increased by addition of LPS and PAM3CSK, addition of the placebo patch has no effect on cytokine levels, whereas treatment with either the prednisolone-containing patch or prednisolone in solution caused a dramatic and significant reduction in all cytokine levels compared to stimulated controls (Fig. 8B). Similar data was produced when THP-1 cells were treated in suspension, in the absence of a GME (Supplementary Fig. 3). These data show that upon release from the patch prednisolone retains its anti-inflammatory properties, even when delivered through a full thickness epithelium.

4. Discussion

Tooth extractions are one of the commonest surgeries with millions
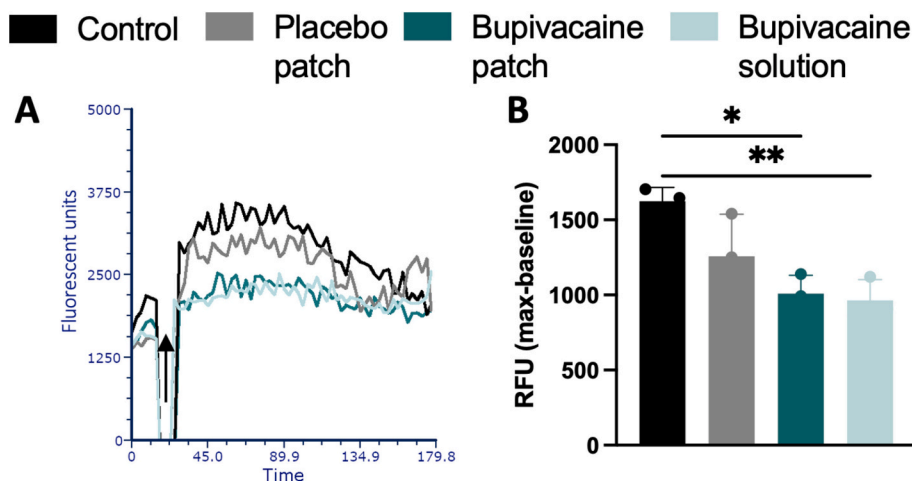
Fig. 7. Bupivacaine remains biologically active following patch release. Untreated control (black), placebo patch eluent (grey), bupivacaine HCl patch eluent (dark teal), bupivacaine HCl solution (345 mM) (turquoise). Calcium flux in SH-SY5Y cells was determined overtime using flow cytometry. Baseline fluorescence was acquired for 10 s before injection of veratridine (black arrow) to induce a calcium influx **(A)**. Relative fluorescent units (RFU) were determined by subtracting the median baseline from the maximum median fluorescence following stimulation with veratridine **(B)**. Data are shown as mean $\pm$ SD, n = 3, for three independent experiments. Statistical significance was determined using an ordinary one-way ANOVA followed by Dunnett's post hoc test with a significance difference indicated by **p* < 0.05, ***p* < 0.01. (For interpretation of the references to colour in this figure legend, the reader is referred to the web version of this article.)
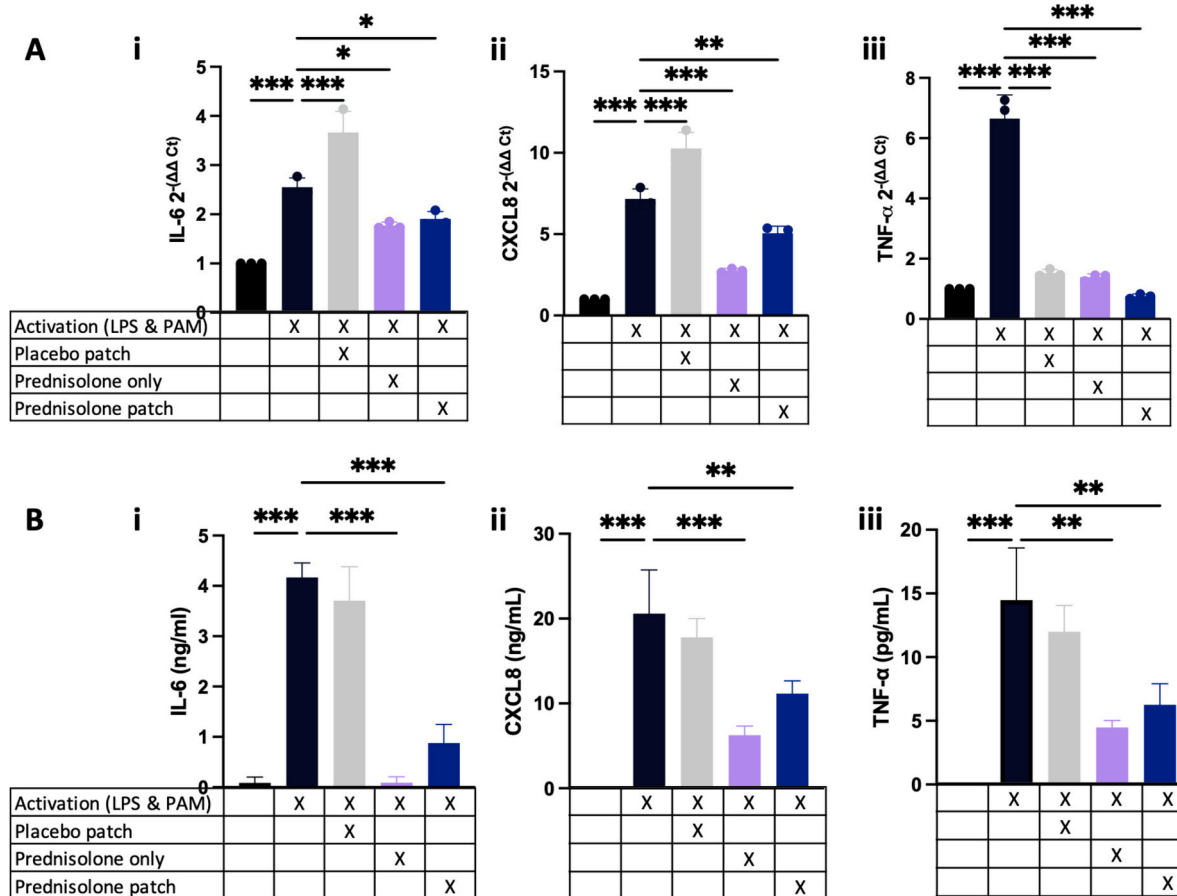
Fig. 8. Prednisolone exhibits anti-inflammatory activity following patch release and permeation through a gingival mucosal equivalent. THP-1 (10^6 cells) contained below a OME were activated with LPS (100 ng) and PAM3CSK (100 ng) for 24 h followed by a 6-h topical treatment with medium alone (negative control), placebo patch, prednisolone patch or prednisolone solution. Gene expression for IL-6 **(Ai)**, CXCL8 **(Aii)** and TNF- α **(Aiii)** were analysed by qPCR, calculated relative to the reference control gene β2-microglobulin and normalised to the untreated control. To measure protein secretion the treatment length, following stimulation, was increased to 24 h for medium only (negative control), placebo patch, prednisolone patch or prednisolone solution. Condition media collected was assayed for inflammatory cytokines IL-6 **(Bi)** CXCL8 **(Bii)** and TNF-α **(Biii)** by ELISA. Data are presented as the mean ± SD, $n = 3$. Statistical significance was determined using an ordinary one-way ANOVA followed by Dunnett's post-hoc test with a significance difference indicated by *$p < 0.05$, **p < 0.01, ***$p < 0.001$.

of procedures carried out worldwide each year. Post-surgical complications such as AO are common yet current treatments or preventative measures for this condition are inadequate. Therefore, the translational potential for new AO treatments is considerable. AO requires a sophisticated therapeutic approach to both protect the extraction site and enable delivery different therapeutic agents at different time intervals post-surgery. Indeed, it is this complexity that has undermined the development of effective interventions to date. Electrospinning technology is increasingly being developed to treat oral conditions such as periodontitis [43], candidiasis [44], premalignant disorders [45,46], oral lichen planus [22,47] and now AO.

The final patch design comprised three layers: the first layer was a blend of dual electrospun PVP (10 % w/v)/RS100 (12 % w/v) fibres loaded with prednisolone along with PNIPAM (5 % w/v) loaded with bupivacaine HCl. The middle layer consisted of PNIPAM (5 % w/v) loaded with bupivacaine HCl alone, which was required to increase bupivacaine content to achieve the desired dose. The final layer consisted of heat-treated PCL to provide a hydrophobic backing later for protection and to drive unidirectional drug delivery into the tissue, preventing drug release into the oral cavity. Confocal microscopy images showed that the PVP/RS100 and PNIPAM fibres form an intimate blend upon use of a mandrel collection plate. This dual fibre patch approach facilitated patch adhesion in a PVP/RS100-dependent manner allowing PNIPAM fibres to also adhere, which was not evident when drug-loaded PNIPAM fibres alone were tested for adherence.

Bupivacaine HCl, tramadol HCl (analgesics), celecoxib, naproxen (COX-2 inhibitor; NSAID) or prednisolone (corticosteroid) were all successfully incorporated into PVP/RS100 electrospun fibres. Addition of bupivacaine HCl and tramadol HCl led to a significant increase in the conductivity of the PVP/RS100 polymer solution, most likely attributable to the HCl salts present in these drugs that enhance conductivity through the addition of electrolytes to the solution [48], an effect that also leads to decreased fibre diameters [49]. Naproxen (an acidic NSAID with a pH range of 2.2–3.7) lowered the pH of the solution, celecoxib, (a non-acidic NSAID), did not affect the pH while the alkaline drugs bupivacaine and tramadol caused an expected increase in pH [50,51]. Upon application to the oral cavity the pH is buffered by bicarbonates within saliva to maintain the local environment at pH 6.7–7.3, thus mitigating fluctuations in pH caused by these patches [52].

The physical properties of the final electrospun patch, including the ability to adhere at the clinical site to stabilise the blood clot, are critical for both protection and targeted drug delivery. All drug-containing patches except tramadol HCl were adhesive for up to 150 h. Patch adhesion primarily relies on PVP that swells upon contact with water, RS100 prevents the rapid dissolution of PVP while permitting the patch to swell [23,53]. The microfiber structure provides a large surface area, and along with water uptake facilitates adhesion through capillary action and osmotic pressure. Sustained adhesion is likely attributed to electrostatic interactions involving the cationic functional groups of RS100, along with hydrogen bonding between both PVP and RS100 to

the mucosa [54].

Naproxen was eliminated due to its low pH while celecoxib was removed due to its likely cross-reactivity with prednisolone, giving rise to gastrointestinal toxicity, bleeding and ulcerogenic potential [55]. Therefore, bupivacaine HCl and prednisolone were chosen. Bupivacaine HCl is quick acting and provides long lasting pain-relief for up to 8 h while anti-inflammatory prednisolone, which has been shown to reduce AO occurrence [56], can take up to 24 h to inhibit proinflammatory mediators and has a duration of action of 8 h. Therefore, an instant but sustained release of prednisolone from electrospun fibres is desirable for prolonged anti-inflammatory effect coupled with a sustained release of bupivacaine HCl to offer an immediate but also longer lasting pain-relief.

Although informative, drug release into PBS is not physiologically relevant, therefore, drug permeation was investigated using in vitro models that mimic the human gingival epithelium [40,57]. Dual spun and drug-loaded patches were non-toxic in line with previous studies on similar patches [22,58]. Upon release both bupivacaine HCl and prednisolone permeated the epithelium, aligning with previous studies on the permeation of other local anaesthetics and corticosteroids [24,22]. It was noted that drug permeation through the epithelium was greater when delivered via a fibre-based system compared to drug delivered in a solution, indicating that fibre-mediated drug delivery is more effective; likely due to the high local concentration of drug at the epithelial surface. Both drugs were delivered in a sustained manner over a 24 h period.

These data show that when delivered in a dual electrospun patch, PNIPAM fibres slow down the release of prednisolone from the PVP/RS100 fibres. This is likely due to the interspersed PNIPAM fibres restricting water uptake and reducing the rate of swelling and drug release from the PVP-RS100 fibres. Once released from the fibres the physicochemical properties of these drugs such as lipophilicity (logP), ionisation and mass may also affect epithelial permeation further.

Patch-released bupivacaine HCl and prednisolone maintained their biological activity. Bupivacaine HCl exerted its anaesthetic activity by blocking voltage-gated sodium channels on SH-SY5Y neuronal cells, as shown previously for lidocaine [24]. Prednisolone suppressed the expression and release of pro-inflammatory cytokines (*IL-6*, *CXCL8* and *TNF-α*) by LPS and PAM3CSK-activated THP-1 monocytes in a full-thickness gingival model. These data provide clear evidence that the levels of bupivacaine HCl and prednisolone released from dual spun patches are therapeutically active, enabling the blockage of oral mucosal neuronal cell depolarisation and preventing inflammation, key requirements for the management of pain and inflammation associated with AO.

5. Conclusions

This is the first detailed report of the fabrication and evaluation of a dual drug-loaded mucoadhesive electrospun patch designed specifically for AO. This study employed simultaneous electrospinning of different drug-polymer systems to produce a novel, adhesive electrospun patch that was able to deliver both analgesic and anti-inflammatory drugs simultaneously. Moreover, these patches provided temporal control of release for different therapeutic agents, further improving potential efficacy. Following release, drugs permeated the gingival mucosa, retained their biological activity and acted upon relevant cells. The translation of this innovative electrospun patch technology to the clinic will be highly impactful, representing a step-change for the effective prevention of AO.

CRediT authorship contribution statement

Klaudia M. Slowik: Writing – review & editing, Writing – original draft, Methodology, Investigation, Formal analysis, Conceptualization. **Jake G. Edmans:** Writing – review & editing, Methodology, Investigation. **Samuel Harrison:** Writing – review & editing, Methodology, Investigation. **Sean M. Edwards:** Writing – review & editing, Methodology. **Robert Bolt:** Writing – review & editing, Supervision, Funding acquisition, Conceptualization. **Sebastian G. Spain:** Writing – review & editing, Supervision, Methodology, Conceptualization. **Paul V. Hatton:** Writing – review & editing, Supervision, Conceptualization. **Craig Murdoch:** Writing – review & editing, Writing – original draft, Supervision, Methodology, Conceptualization. **Helen E. Colley:** Writing – original draft, Supervision, Project administration, Methodology, Funding acquisition, Conceptualization.

Declaration of Competing Interest

PVH is a scientific advisor to AFYX. CM, HEC, JGE, SGS have all previously received funding from AFYX, although AFYX did not fund any part of this work.

Data availability

Data will be made available on request.

Acknowledgements

Appendix A. Supplementary data

Supplementary data to this article can be found online at https://doi.org/10.1016/j.jconrel.2024.09.048.

References

[1] O. Chow, R. Wang, D. Ku, W. Huang, Alveolar osteitis: a review of current concepts, J. Oral Maxillofac. Surg. 78 (2020) 1288–1296.

[2] B.J. Daly, M.O. Sharif, K. Jones, H.V. Worthington, A. Beattie, Local interventions for the management of alveolar osteitis (dry socket), Cochrane Database Syst. Rev. 9 (2022) CD006968.

[3] National-Health-Service, FOI 01535 Extractions 2017–2023, The National Archives (on-line), 2024.

[4] J.W. Friedman, The prophylactic extraction of third molars: a public health hazard, Am. J. Public Health 97 (2007) 1554–1559.

[5] A. Ghosh, V.R. Aggarwal, R. Moore, Aetiology, prevention and management of alveolar osteitis - a scoping review, J. Oral Rehabil. 49 (2022) 103–113.

[6] W. Kusnierek, K. Brzezinska, K. Nijakowski, A. Surdacka, Smoking as a risk factor for dry socket: a systematic review, Dent. J. (Basel) 10 (2022).

[7] V. Rakhshan, Common risk factors of dry socket (alveolitis osteitis) following dental extraction: a brief narrative review, J. Stomatol. Oral Maxillofac Surg. 119 (2018) 407–411.

[8] A.G. Garcia, P.M. Grana, F.G. Sampedro, M.P. Diago, J.M. Rey, Does oral contraceptive use affect the incidence of complications after extraction of a mandibular third molar? Br. Dent. J. 194 (2003) 453–455, discussion 445.

[9] M. Penarrocha, J.M. Sanchis, U. Saez, C. Gay, J.V. Bagan, Oral hygiene and postoperative pain after mandibular third molar surgery, Oral Surg. Oral Med. Oral Pathol. Oral Radiol. Endod. 92 (2001) 260–264.

[10] F. Garola, G. Gilligan, R. Panico, N. Leonardi, E. Piemonte, Clinical management of alveolar osteitis. A systematic review, Med. Oral Patol. Oral Cir. Bucal. 26 (2021) e691–e702.

[11] M.R. Poor, J.E. Hall, A.S. Poor, Reduction in the incidence of alveolar osteitis in patients treated with the SaliCept patch, containing Acemannan hydrogel, J. Oral Maxillofac. Surg. 60 (2002) 374–379 (discussion 379).

[12] J.F. Silvestre, M.P. Albares, M. Blanes, J.C. Pascual, N. Pastor, Allergic contact gingivitis due to eugenol present in a restorative dental material, Contact Derm. 52 (2005) 341.

[13] M. Eshghpour, P. Dastmalchi, A.H. Nekooei, A. Nejat, Effect of platelet-rich fibrin on frequency of alveolar osteitis following mandibular third molar surgery: a double-blinded randomized clinical trial, J. Oral Maxillofac. Surg. 72 (2014) 1463–1467.

[14] A. Sharma, N. Aggarwal, S. Rastogi, R. Choudhury, S. Tripathi, Effectiveness of platelet-rich fibrin in the management of pain and delayed wound healing associated with established alveolar osteitis (dry socket), Eur. J. Dent. 11 (2017) 508–513.

[15] H.M. Asmael, F.A. Jamil, A.M. Hasan, Novel application of platelet-rich fibrin as a wound healing enhancement in extraction sockets of patients who smoke, J. Craniofac. Surg. 29 (2018) e794–e797.

[16] S. Chakravarthi, Platelet rich fibrin in the management of established dry socket, J. Korean Assoc. Oral Maxillofac. Surg. 43 (2017) 160–165.

[17] M.A. Isiordia-Espinoza, O.H. Aragon-Martinez, R.E. Bollogna-Molina, A.J. Alonso-Castro, Infection, alveolar osteitis, and adverse effects using metronidazole in healthy patients undergoing third molar surgery: a meta-analysis, J. Maxillofac. Oral. Surg. 17 (2018) 142–149.

[18] S. Sidana, Y. Mistry, A. Gandevivala, N. Motwani, Evaluation of the need for antibiotic prophylaxis during routine intra-alveolar dental extractions in healthy patients: a randomized double-blind controlled trial, J. Evid. Based Dent. Pract. 17 (2017) 184–189.

[19] A. Haraji, V. Rakhshan, Single-dose intra-alveolar chlorhexidine gel application, easier surgeries, and younger ages are associated with reduced dry socket risk, J. Oral Maxillofac. Surg. 72 (2014) 259–265.

[20] J.T. Murph Jr., S.H. Jaques, A.N. Knoell, G.D. Archibald, S. Yang, A retrospective study on the use of a dental dressing to reduce dry socket incidence in smokers, Gen. Dent. 63 (2015) 17–21.

[21] A. Kilinc, H. Ataol, How effective is collagen resorbable membrane placement after partially impacted mandibular third molar surgery on postoperative morbidity? A prospective randomized comparative study, BMC Oral. Health 17 (2017) 126.

[22] H.E. Colley, Z. Said, M.E. Santocildes-Romero, S.R. Baker, K. D'Apice, J. Hansen, L. S. Madsen, M.H. Thornhill, P.V. Hatton, C. Murdoch, Pre-clinical evaluation of novel mucoadhesive bilayer patches for local delivery of clobetasol-17-propionate to the oral mucosa, Biomaterials 178 (2018) 134–146.

[23] M.E. Santocildes-Romero, L. Hadley, K.H. Clitherow, J. Hansen, C. Murdoch, H. E. Colley, M.H. Thornhill, P.V. Hatton, Fabrication of electrospun mucoadhesive membranes for therapeutic applications in oral medicine, ACS Appl. Mater. Interfaces 9 (2017) 11557–11567.

[24] K.H. Clitherow, C. Murdoch, S.G. Spain, A.M. Handler, H.E. Colley, M.B. Stie, H. Morck Nielsen, C. Janfelt, P.V. Hatton, J. Jacobsen, Mucoadhesive electrospun patch delivery of lidocaine to the oral mucosa and investigation of spatial distribution in a tissue using MALDI-mass spectrometry imaging, Mol. Pharm. 16 (2019) 3948–3956.

[25] A. Nikam, P.R. Sahoo, S. Musale, R.R. Pagar, A.C. Paiva-Santos, P.S. Giram, A systematic overview of Eudragit((R))-based copolymer for smart healthcare, Pharmaceutics 15 (2023).

[26] A.K.D. Garkal, S. Musale, T. Mehta, P. Giram, Electrospinning nanofiber technology: a multifaceted paradigm in biomedical application, New J. Chem. 45 (2021) 21508–21533.

[27] D.G. Yu, W. Gong, J. Zhou, Y. Liu, Y. Zhu, X. Lu, Engineered shapes using electrohydrodynamic atomization for an improved drug delivery, Wiley Interdiscip. Rev. Nanomed. Nanobiotechnol. 16 (2024) e1964.

[28] Z. Zhang, H. Liu, D.G. Yu, S.A. Bligh, Alginate-based electrospun nanofibers and the enabled drug controlled release profiles: a review, Biomolecules 14 (2024).

[29] A.C.B. Allen, E. Barone, C.O.K. Crosby, L.J. Suggs, J. Zoldan, Electrospun poly(N-isopropyl acrylamide)/poly(caprolactone) fibers for the generation of anisotropic cell sheets, Biomater. Sci. 5 (2017) 1661–1669.

[30] Y.C. Chuang, Y.C. Chang, M.T. Tsai, T.W. Yang, M.T. Huang, S.H. Wu, C. Wang, Electrospinning of aqueous solutions of atactic poly(N-isopropylacrylamide) with physical gelation, Gels 8 (2022).

[31] X. Xu, Y. Liu, W. Fu, M. Yao, Z. Ding, J. Xuan, D. Li, S. Wang, Y. Xia, M. Cao, Poly (N-isopropylacrylamide)-based thermoresponsive composite hydrogels for biomedical applications, Polymers (Basel) 12 (2020).

[32] V.Y.D.A.S. Grinberg, D.V. Kuznetsov, N.V. Grinberg, A. Grosberg, T. Tanaka, Studies of the thermal volume transition of poly(N-isopropylacrylamide) hydrogels by high-sensitivity differential scanning microcalorimetry. 2, Thermodyn. Funct. Macromol. 33 (2000) 8685–8692.

[33] T.H.M. Tran, D. Patel, E. Burns, V. Peterman, J. Wu, Controllable and switchable drug delivery of ibuprofen from temperature responsive composite nanofibers, Nano Convergen. 2 (2015).

[34] Z. Wei, W. Zhao, Y. Wang, X. Wang, S. Long, J. Yang, Novel PNIPAm-based electrospun nano fi bres used directly as a drug carrier for "on-off" switchable drug release, Colloids Surf. B: Biointerfaces 182 (2019) 110347.

[35] J.G. Edmans, K.H. Clitherow, C. Murdoch, P.V. Hatton, S.G. Spain, H.E. Colley, Mucoadhesive electrospun fibre-based technologies for oral medicine, Pharmaceutics 12 (2020).

[36] J.G. Edmans, S. Harrison, P.V. Hatton, C. Murdoch, S.G. Spain, H.E. Colley, Electrospinning polymersomes into bead-on-string polyethylene oxide fibres for the delivery of biopharmaceuticals to mucosal epithelia, Biomat. Adv. 157 (2024) 213734.

[37] K. Lindberg, J.G. Rheinwald, Three distinct keratinocyte subtypes identified in human oral epithelium by their patterns of keratin expression in culture and in xenografts, Differentiation 45 (1990) 230–241.

[38] S. Tsuchiya, M. Yamabe, Y. Yamaguchi, T. Konno, K. Tada, Establishment and characterization of a human scute monocytic leukemia cell line (THP-1), Int. J. Cancer 26 (1980) 171.

[39] J.L. Biedler, S. Roffler-Tarlov, M. Schachner, L.S. Freedman, Multiple neurotransmitter synthesis by human neuroblastoma cell lines and clones, Cancer Res. 38 (1978) 3751–3757.

[40] J.K. Buskermolen, C.M. Reijnders, S.W. Spiekstra, T. Steinberg, C.J. Kleverlaan, A. J. Feilzer, A.D. Bakker, S. Gibbs, Development of a full-thickness human gingiva equivalent constructed from immortalized keratinocytes and fibroblasts, Tissue Eng. Part C Methods 22 (2016) 781–791.

[41] W. Ulbricht, Effects of veratridine on sodium currents and fluxes, Rev. Physiol. Biochem. Pharmacol. 133 (1998) 1–54.

[42] I. Vetter, C.A. Mozar, T. Durek, J.S. Wingerd, P.F. Alewood, M.J. Christie, R. J. Lewis, Characterisation of Na(v) types endogenously expressed in human SH-SY5Y neuroblastoma cells, Biochem. Pharmacol. 83 (2012) 1562–1571.

[43] P.Z.K. Zhao, Y. Xia, C. Qian, D.G. Yu, Y. Xie, Y. Liao, Electrospun trilayer eccentric Janus nanofibers for a combined treatment of periodontitis, Adv. Fiber Mater. 6 (2024) 1053–1073.

[44] K.H. Clitherow, T.M. Binaljadm, J. Hansen, S.G. Spain, P.V. Hatton, C. Murdoch, Medium-chain fatty acids released from polymeric electrospun patches inhibit Candida albicans growth and reduce the biofilm viability, ACS Biomater. Sci. Eng. 6 (2020) 4087–4095.

[45] X. Liu, Q. Li, Y. Wang, M. Crawford, P.K. Bhupal, X. Gao, H. Xie, D. Liang, Y. L. Cheng, X. Liu, R.Y.L. Tsai, Designing a mucoadhesive chemopatch to ablate oral dysplasia for cancer prevention, Small 18 (2022) e2201561.

[46] H.J.Y. Zhang, C. Yuan, P. Sun, Q. Xu, D. Lin, Z. Han, X. Xu, Q. Zhou, J. Deng, Fabrication of astaxanthin-loaded electrospun nanofiber-based mucoadhesive patches with water-insoluble backing for the treatment of oral premalignant lesions, Mater. Des. 223 (2022) 111311.

[47] J.G. Edmans, B. Ollington, H.E. Colley, M.E. Santocildes-Romero, L. Siim Madsen, P.V. Hatton, S.G. Spain, C. Murdoch, Electrospun patch delivery of anti-TNF-alpha F(ab) for the treatment of inflammatory oral mucosal disease, J. Control. Release 350 (2022) 146–157.

[48] K. Karami, N. Merclin, F. Brouneus, P. Beronius, On iontophoretic delivery enhancement: ionization and transport properties of lidocaine hydrochloride in aqueous propylene glycol, Int. J. Pharm. 201 (2000) 121–124.

[49] C.J.J.S.H. Angammana, Analysis of the effects of solution conductivity on electrospinning process and fiber morphology, IEEE Trans. Ind. Appl. 47 (2011) 1109–1117.

[50] M. Mabrouk, H.H. Beherei, S. ElShebiney, M. Tanaka, Newly developed controlled release subcutaneous formulation for tramadol hydrochloride, Saudi Pharm. J. 26 (2018) 585–592.

[51] J.C.M.M. Shah, pH-dependent solubility and dissolution of bupivacaine and its relevance to the formulation of a controlled release system, J. Control. Release 23 (1993) 261–270.

[52] D.J. Aframian, T. Davidowitz, R. Benoliel, The distribution of oral mucosal pH values in healthy saliva secretors, Oral Dis. 12 (2006) 420–423.

[53] S. Tort, A. Yildiz, F. Tugcu-Demiroz, G. Akca, O. Kuzukiran, F. Acarturk, Development and characterization of rapid dissolving ornidazole loaded PVP electrospun fibers, Pharm. Dev. Technol. 24 (2019) 864–873.

[54] P.D.S. Chaves, L.A. Frank, A.G. Frank, A.R. Pohlmann, S.S. Guterres, R.C.R. Beck, Mucoadhesive properties of Eudragit(R)RS100, Eudragit(R)S100, and poly (epsilon-caprolactone) nanocapsules: influence of the vehicle and the mucosal surface, AAPS PharmSciTech 19 (2018) 1637–1646.

[55] E.E. Moore, H.B. Moore, E. Gonzalez, M.P. Chapman, K.C. Hansen, A. Sauaia, C. C. Silliman, A. Banerjee, Postinjury fibrinolysis shutdown: rationale for selective tranexamic acid, J. Trauma Acute Care Surg. 78 (2015) S65–S69.

[56] W.C. Ngeow, D. Lim, Do corticosteroids still have a role in the management of third molar surgery? Adv. Ther. 33 (2016) 1105–1139.

[57] B. Srinivasan, A.R. Kolli, M.B. Esch, H.E. Abaci, M.L. Shuler, J.J. Hickman, TEER measurement techniques for in vitro barrier model systems, J. Lab. Autom. 20 (2015) 107–126.

[58] O. Groborz, K. Kolouchova, J. Pankrac, P. Kesa, J. Kadlec, T. Krunclova, A. Pierzynova, J. Sramek, M. Hovorakova, L. Dalecka, Z. Pavlikova, P. Matous, P. Paral, L. Loukotova, P. Svec, H. Benes, L. Stepanek, D. Dunlop, C.V. Melo, L. Sefc, T. Slanina, J. Benes, S. Van Vlierberghe, R. Hoogenboom, M. Hruby, Pharmacokinetics of intramuscularly administered thermoresponsive polymers, Adv. Healthc. Mater. 11 (2022) e2201344.